Research Article
Vol. 26, No. 9 | 30 Apr 2018 | OPTICS EXPRESS 11649
Optics EXPRESS

# Through-focus scanning optical microscopy with the Fourier modal method

SHIN-WOONG PARK,[1] GYUNAM PARK,[2] YOUNGBAEK KIM,[3] JOONG HWEE CHO,[3] JUNHO LEE,[2,5] AND HWI KIM[1,4,*]

[1]*ICT Convergence Technology for Health & Safety, Korea University, 2511 Sejong-ro, Sejong 30019, South Korea*
[2]*Department of Optical Engineering, Kongju National University, 1223-24 Cheonan-daero, Seobuk-gu, Cheonan 31080, South Korea*
[3]*Department of Embedded Systems Engineering, Incheon National University, 119 Academy-ro, Yeonsu-gu, Incheon 22012, South Korea*
[4]*Department of Electronics and Information Engineering, Korea University, 2511 Sejong-ro, Sejong 30019, South Korea*
[5]*jhlsat@kjnu.ac.kr*
[*]*hwikim@korea.ac.kr*

**Abstract:** We propose a Fourier modal method (FMM) based through-focus scanning optical microscopy (TSOM) featuring sub-nano scale measurement tolerance. TSOM is very recently conceptualized non-destructive optical metrology technique just at the beginning stage of research. Nowadays the reliability and feasibility of TSOM concept is subject to controversy. We experimentally demonstrate stable nano-scale metrology of the FMM-based TSOM for the verification of the TSOM metrology and provide a numerical tool for true nano-meter scale TSOM through devising the FMM based TSOM scheme. By considering the illumination light parameters of incidence angle, polarization, degree of coherence, illumination numerical aperture, and collection numerical apertures in the FMM modeling of TSOM image acquisition, we reach precise agreement between the calculated and experimentally measured TSOM images. The essential elements of the FMM based TSOM for achieving high-level consistency are elucidated.



**OCIS codes:** (120.0120) Instrumentation, measurement, and metrology; (180.0180) Microscopy; (050.1755) Computational electromagnetic methods; (260.2110) Electromagnetic optics.

## References and links

1. R. Attota, R. Dixson, and A. Vladár, "Through-focus scanning optical microscopy," Proc. SPIE **8036**, 803610 (2011).
2. R. Attota, R. Dixson, J. Kramar, J. Potzick, A. Vladár, B. Bunday, E. Novak, and A. Rudack, "TSOM method for semiconductor metrology," Proc. SPIE **7971**, 79710T (2011).
3. A. Arceo, B. Bunday, V. Vartanian, and R. Attota, "Patterned defect and CD metrology by TSOM beyond the 22 nm node," Proc. SPIE **8324**, 83240E (2012).
4. R. K. Attota and H. Kang, "Parameter optimization for through-focus scanning optical microscopy," Opt. Express **24**(13), 14915–14924 (2016).
5. M. Pisarenco and I. Setija, "Alternative discretization in the aperiodic Fourier modal method leading to reduction in computational costs," Proc. SPIE **8789**, 87890K (2013).
6. H. Kim and B. Lee, "Mathematical modeling of crossed nanophotonic structures with generalized scattering-matrix method and local Fourier modal analysis," J. Opt. Soc. Am. B **25**(4), 518–544 (2008).
7. H. Kim and B. Lee, "Pseudo-Fourier modal analysis of two-dimensional arbitrarily shaped grating structures," J. Opt. Soc. Am. A **25**(1), 40–54 (2008).
8. H. Kim, I. M. Lee, and B. Lee, "Extended scattering-matrix method for efficient full parallel implementation of rigorous coupled-wave analysis," J. Opt. Soc. Am. A **24**(8), 2313–2327 (2007).
9. H. Kim, G. Park, and C. Kim, "Investigation of the convergence behavior with fluctuation features in the Fourier modal analysis of a metallic grating," J. Opt. Soc. Korea **16**(3), 196–202 (2012).
10. H. Kim, Junghyun Park, and Byoungho Lee, *Fourier Modal Method and Its Applications in Computational Nanophotonics* (CRC, 2012).

#325280 https://doi.org/10.1364/OE.26.011649
Journal © 2018 Received 2 Mar 2018; revised 7 Apr 2018; accepted 9 Apr 2018; published 20 Apr 2018

Optics EXPRESS

11. M. V. Ryabko, S. N. Koptyaev, A. V. Shcherbakov, A. D. Lantsov, and S. Y. Oh, "Method for optical inspection of nanoscale objects based upon analysis of their defocused images and features of its practical implementation," Opt. Express **21**(21), 24483–24489 (2013).
12. M. Ryabko, A. Shchekin, S. Koptyaev, A. Lantsov, A. Medvedev, A. Shcherbakov, and S. Y. Oh, "Through-focus scanning optical aberrations: practical implementation," Opt. Express **23**, 32215–32221 (2015).
13. R. Attota and J. Kramar, "Optimizing noise for defect analysis with through-focus scanning optical microscopy," Proc SPIE Int Soc Opt Eng **9778**, 977811 (2016).
14. R. K. Attota, P. Weck, J. A. Kramar, B. Bunday, and V. Vartanian, "Feasibility study on 3-D shape analysis of high-aspect-ratio features using through-focus scanning optical microscopy," Opt. Express **24**(15), 16574–16585 (2016).
15. J. Qin, R. M. Silver, B. M. Barnes, H. Zhou, R. G. Dixson, and M.-A. Henn, "Deep subwavelength nanometric image reconstruction using Fourier domain optical normalization," Light Sci. Appl. **5**, e16038 (2016).
16. R. K. Attota and H. Park, "Optical microscope illumination analysis using through-focus scanning optical microscopy," Opt. Lett. **42**(12), 2306–2309 (2017).

## 1. Introduction

Through-focus scanning optical microscopy (TSOM) is an optical microscopic inspection and metrology technique for three-dimensional (3D) nanoscale semiconductor structures such as high-aspect ratio through silicon via (TSV) and fin field-effect transistors (Fin-FETs). Conventional high-NA microscopes are limited in their transversal resolution and depth-of-focus (DOF) when measuring nanoscale high-aspect ratio structures. The development of TSOM is motivated for application to in-line non-destructive inspection and measurement of such high-aspect ratio and subwavelength nano-scale structures in state of the art semiconductor devices [1,2]. The TSOM method differs from conventional optical microscopy in that it indirectly measures deep-subwavelength structures based on computational interpretation of far-field TSOM images [3].

The TSOM images measured from subwavelength target structures are compared with the numerically calculated TSOM reference image and analyzed in terms of their differential TSOM features. The structural difference that induces the differential TSOM image features can be determined by numerically classifying the target samples with respect to nanometer scale structural variations in the prepared TSOM image database. To quantify this TSOM analysis, several quantitative measurement factors have been developed including optical intensity range (OIR), different TSOM image (DTI), and mean square difference (MSD) [1,3]. In practice, the construction of the numerical TSOM reference database is the essential part, so TSOM image modeling is of paramount importance. To build up the TSOM reference image database, an efficient and accurate TSOM image calculation engine should be prepared and calibrated correctly to reflect the physical parameters of the experimental optical measurement equipment.

This paper shows that careful consideration of the coherence of the illumination light, the input numerical aperture and the collection numerical aperture of the microscope objective, and the illumination angle are the critical factors for successful TSOM metrology. For this purpose, several tools such as finite-difference time-domain (FDTD) and finite element method (FEM) can be used [1–4]. The TSOM technique preserves all the optical information by capturing in and around the focus position the scattered field reflected off the target in the form of an image containing the target features and moves the target sample to build an overall intensity map of the target. Thus, the intensity calculation of the TSOM image using FDTD or FEM have carried out repetitively with the movement of the target. However, in the buildup of the reference TSOM image database, the TSOM image generation with 0.1nm or smaller step changes in structural parameters should be afforded by the numerical modeling engine. The fine structural parameter change is limited in spatial domain method such as FDTD and FEM since both methods are based on the spatial discrete computation grid. The structural change is discretized and the parametric TSOM image generation with fine steps increases the required computational resource dramatically and degrades the computational efficiency of the reference TSOM image database.

This paper proposes that for TSOM the Fourier modal method (FMM) is the optimal numerical modeling methodology. FMM is a well-known frequency domain method for Maxwell equations. The efficiency of TSOM image reference buildup can be improved by representing the Maxwell equations in the frequency domain using Fourier transform and calculating the scattering matrix of the target sample structure [5–10]. Using the FMM requires that the frequency domain is discretized, but a range of spatial domain parameters can be dealt with in a continuous support accurately and efficiently. Even after the refinement of the structural parameter sampling steps, the computational resources required can remain stable. The inclusion of experimentally reliable physical parameters such as any real number incidence angle or degree of coherence into the simulation code is easy in practice. The calculated scattering matrix can be obtained once and then simply applied to obtain field distributions related to *z*-axis sample position change without repetitive Maxwell equation calculation. Those theoretical advantages make FMM a very appropriate and versatile tool for TSOM technology.

This paper is organized as follows. In section 2, the FMM-TSOM modeling of a simple nanoscale semiconductor structure is described with comparison to the FDTD-TSOM modeling of a previous paper [3]. In section 3, the meteorological performance of the proposed FMM-TSOM measurement is validated experimentally and its numerical performance is verified in terms of efficiency, flexibility and accuracy. The simulated and experimental results are then compared to verify the consistency of the proposed method for MSD evaluation. Finally, concluding remarks are presented in section 4.

## 2. FMM modeling of TSOM under finite NA incoherent illumination

For successful TSOM metrology, the parameters of the optical microscope for TSOM sensitivity such as the illumination and collection numerical apertures (NAs) and the illumination angle must be exactly quantified [1–3]. The meanings of illumination NA (INA) and collection NA (CNA) are schematically illustrated in Fig. 1(a), and Fig. 1(b) shows that each scan position results in a slightly different two-dimensional intensity image. The serial compilation of those section-wise intensity profiles turns into TSOM image. The relationship between INA and CNA requires optimization and is linked to the optical degree of coherence of illumination. It is known that the sensitivity of TSOM can be enhanced by optimizing the INA and CNA [3].

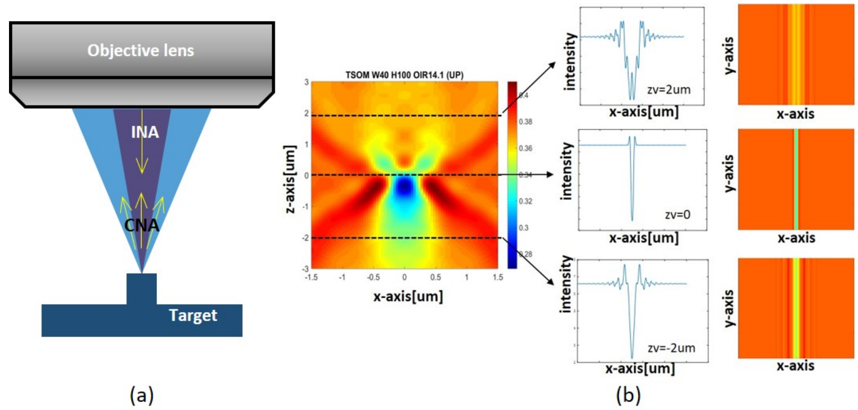


Fig. 1. (a) Schematic of an objective showing illumination and collection NAs, (b) the method of constructing a TSOM image; intensity profiles of dotted lines in the left figure and their respective cross-sectional images

A decrease in INA leads to an interference or diffraction optical signal in TSOM images [5,11–14] due to increased optical coherence of the illuminating field. However, the influence

Optics EXPRESS

of the degree of coherence has not been well studied and remains an unexplored research topic. From the results of [5], the OIR of the TSOM, as well as the DTIs, increase with decreasing INA, showing that TSOM sensitivity increases with decreasing INA.

Most of all, incoherent illumination modeling is relatively easy and efficient for the FMM [15]. Since the FMM is a plane-wave based frequency domain method, the finite NA illumination field is represented by the sum of the elementary plane waves with different k-vectors as schematically illustrated in Figs. 2(a) and 2(b). In the FMM, the *k*-vector spectrum is discretized by $k_{x,m} = 2\pi m / T_x$, where $T_x$ is the *x*-directional computational grid dimension used for the FMM calculation and $m$ is an integer. This discretization scheme can be straightforwardly extended to a three-dimensional FMM calculation using $\left(k_{x,m}, k_{y,n}\right) = \left(2\pi m / T_x, 2\pi n / T_y\right)$, where $T_y$ is the *y*-directional computational grid dimension used for the FMM calculation and $n$ is an integer.

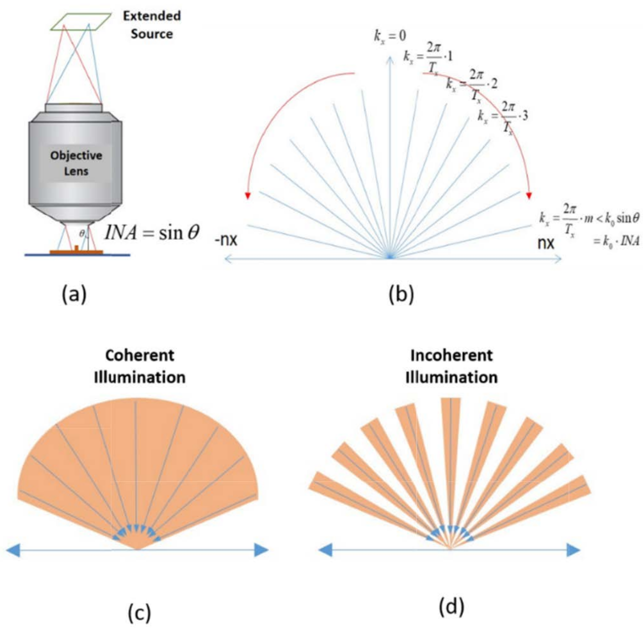


Fig. 2. (a) Finite NA illumination light for TSOM imaging. (b) Angular spectrum representations of (c) coherent illumination and (d) incoherent illumination.

The coherent illuminating field is expressed by the angular spectrum integral,

$$E_{x(y,z)}\left(x,y,z\right) = \iint\limits_{\alpha^2+\beta^2 \le \left(1/\lambda NA_{illum}\right)^2} A_{x(y,z)}\left(\alpha,\beta\right) e^{j2\pi\left(\alpha x+\beta y+\sqrt{(1/\lambda)^2-\alpha^2-\beta^2}z\right)} d\alpha d\beta, \quad (1)$$

where $E_x$, $E_y$, and $E_z$ are the *x*, *y*, and *z*-directional electric field components in the free space domain and the angular spectrum coefficients satisfy the plane wave condition,

$$\alpha A_x\left(\alpha,\beta\right) + \beta A_y\left(\alpha,\beta\right) + \sqrt{\left(1/\lambda\right)^2 - \alpha^2 - \beta^2}\, A_z\left(\alpha,\beta\right) = 0. \quad (2)$$

The FMM calculates the reflection and transmission fields $E_{Rx(y,z)}$ and $E_{Tx(y,z)}$ in vector field form for the illuminating field. The coherent field response is schematically illustrated in Fig. 2(c).

The incoherent illumination condition in the FMM represents that each plane wave component is statistically incoherent. Accordingly, the reflection and transmission fields of each illuminating wave component are also incoherent to each other as schematically illustrated in Fig. 2(d). Let us consider the *g*th illuminating component, and denote the reflection and transmission optical field distributions by $E_{r,g}$ and $E_{t,g}$, respectively. For an incoherent illumination plane wave bundle with a finite INA, the total reflection and transmission fields can be respectively modeled as the spatial incoherent accumulation of the field components taking the following forms:

$$\left|E_r\right| = \sqrt{\sum_g \left|E_{r,g}\right|^2}, \tag{3}$$

$$\left|E_t\right| = \sqrt{\sum_g \left|E_{t,g}\right|^2}. \tag{4}$$

Here, it is argued that the incoherent reflection field distribution, $\left|E_r\right| = \sqrt{\sum_k \left|E_{r,k}\right|^2}$, is taken as the TSOM image. According to Fig. 2(d), the incoherent illumination field is modeled by

$$E_{x(y,z)}\left(x,y,z\right) = \iint_{\alpha^2+\beta^2 \le \left(1/\lambda NA_{illum}\right)^2} \left| A_{x(y,z)}\left(\alpha,\beta\right) e^{j2\pi\left(\alpha x+\beta y+\sqrt{\left(1/\lambda\right)^2-\alpha^2-\beta^2}\,z\right)} \right| d\alpha d\beta. \tag{5}$$

Figure 3 presents the comparative simulation results of the TSOM images obtained by the FMM and the FDTD. The FDTD simulation results in Fig. 3(a) were obtained from the previous research [2]. The TSOM images for two targets with a 1.0 nm difference in line width are simulated with a 0.4 illumination NA, 0.8 collection NA, and 546nm illumination wavelength (refractive index = 3.1898 + 0.0036i). The aforementioned incoherent illumination condition is implemented in the TSOM simulation of Fig. 3(b). The proposed FMM scheme can also generate the similar TSOM images as the FDTD that was demonstrated in ref [2].

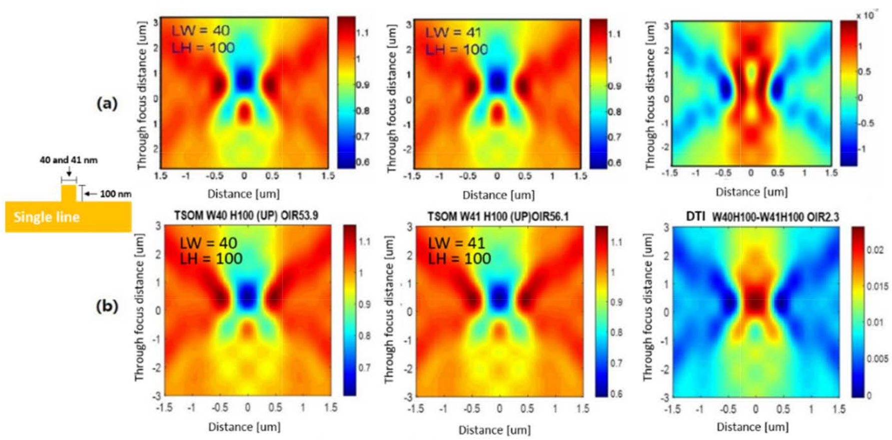


Fig. 3. TSOM images with different fin width and their DTI (a) results from ref [2]. (b) calculated using FMM of this work.

As shown in Fig. 3(b), the optical intensity range (OIR) varies from 53.9 to 56.1 due to a structural change of 1 nm and the DTI in the right side of Fig. 3(b) can be obtained using these images. Some apparent differences between the FMM and FDTD TSOM images are inferred to be caused by mismatches in some optical simulation parameters that are not precisely defined in [2].

The FMM, being a frequency domain method, has a mathematical framework based on the scattering-matrix method in the vectorial angular spectrum domain, and thus is very effective at the SMM computation. Theoretically, all the aspects of the TSOM analysis can be interpreted from the scattering-matrix characterization of the target structures [8–10]. The scattering matrix is the electromagnetic system response operator, that is, the collection of reflection spectra for all possible different directional plane wave incidences. Note that once the scattering matrix is obtained, TSOM images can be efficiently calculated despite changes in INA, CNA, and even the degree of coherence without repetitive recomputation of Maxwell equations. Thus the scattering matrix can be considered to include the complete information set necessary for TSOM image construction. In contrast, the FDTD is considered to require heavily repetitive calculation for all directional plane wave incidence [10] being necessary in the construction of the same SMM.

## 3. Experimental results of FMM-TSOM metrology

We carried out the FMM-TSOM metrology feasibility test for a simple single fin structure target sample. Figure 4 depicts the FMM-TSOM experimental setup, which includes a photographic inset of the real system, and where the illumination system and measurement beam lines share a single objective lens.

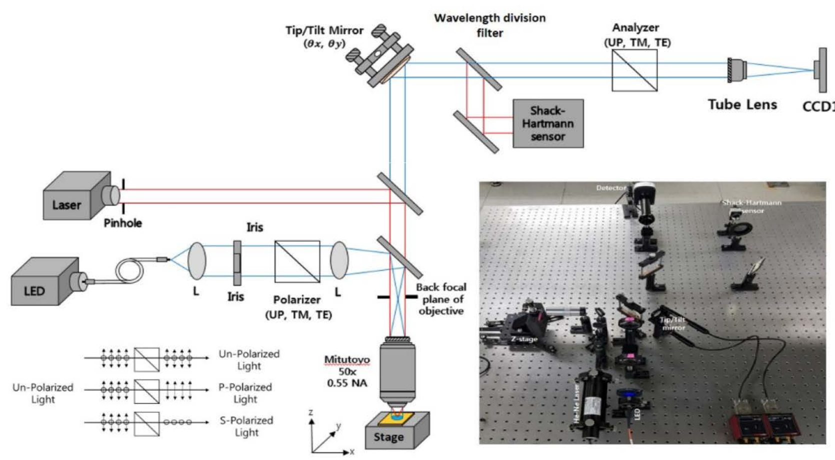


Fig. 4. The experimental setup of the FMM-TSOM metrology. INA and CNA are set to 0.275 and 0.55, respectively.

It was adjusted to hold the illumination NA of 0.275 and the collection NA of 0.55. In the illumination beam line, Köhler illumination with a 470nm LED lamp was implemented to shed uniform unpolarized incident light onto the target samples, while in the measurement beam line, a conventional optical microscope objective lens (50 × Mitutoyo of 4 mm focal length and 0.55 NA) and a tube lens with a 200 mm focal length are used to implement a 50 × microscope system. In order to prevent artifacts caused by the $z$-axis movement, a Shack-Hartmann sensor and a tip/tilt mirror were employed, which can correct the plausible horizontal shift in each z-step movement by measuring the horizontal position of the target sample in real-time [16]. The tilt/tip mirrors was used to stabilize the illumination angle (for example, 10 degree) to nearly constant value against the z-axis movement, not to exact 0 degree of normal incidence. In this research, we found that the strict normal incidence condition of illumination light is not a critical factor for TSOM measurement. In our benchtop experimental system, the alignment of exact 0 degree illumination is quite cumbersome.

Instead, we would like to show that the incidence angle is not a critical factor in the TSOM measurement but a flexible factor. And, during the TSOM image data acquisition, a through-focus step of 200 nm and a total scan range of 20 um were used. The microscopy USB2.0 camera (INFINITY 2-1R) with 1392x1040 pixels was used to take TSOM images. In the experiment, two samples with a single fin line on a Si oxide wafer with 140 and 160 nm widths respectively, and the same 50 nm height, and 100 um length were prepared and their TSOM images captured. The left panels of Figs. 5(a) and 6(a) present the experimental TSOM images of the single line samples with 140 and 160 nm widths, respectively. The middle panels of Figs. 5(a) and 6(a) show the respective numerical TSOM images through the CCD system under the same physical conditions calculated using the proposed FMM-TSOM modeling process. It is important to reflect the inclination of the incident light in the TSOM image calculation. In the experimental TSOM images in Figs. 5(a) and 6(a), the angle of incidence was estimated to be about 10 degrees, and an effective INA of 0.275 and CNA of 0.55 were applied in the FMM calculation. The estimation of the effective INA and CNA were analyzed using ZEMAX software and further refined through the adjustment of the INA and CNA parameters in the FMM TSOM image calculation to achieve the optimal matching of the calculated and experimented TSOM images. In the experimental TSOM images, a non-uniform background intensity distribution is observed along the vertical axis, which is inferred to be caused by the LED light source non-homogeneity. The tip-tilt technique was used to stabilize the inclination of the incident light and the physical wobble on the z-stage movement. In the right panels of Figs. 5(a) and 6(a), the differential TSOM images (DTIs) of the target structures of respective 140 and 160 nm width are shown with the calculated mean squared difference (MSD), which can be used to quantify the magnitude of the difference of the measured and simulated TSOM images given physical parameter change. The MSD is defined as,

$$MSD = \frac{1}{N}\sum_{i=1}^{N}\left(\mathrm{TSOM}_{\mathrm{simulation}} - \mathrm{TSOM}_{\mathrm{experiment}}\right)^2. \qquad (6)$$

In Fig. 5(b) and 6(b), the test results of the sub-nanometer scale metrology of the respective samples is presented. The numerical TSOM images featuring sub-nanoscale linewidth variations are compared with the experimentally measured TSOM image of the target sample in terms of the MSD. The numerical reference TSOM images are considered as a numerical TSOM database with fine structural parameter variation. This capability of near continuous parameter change in the structural modeling and the lack of a need for additional computational resource adjustment when calculating the TSOM image in spite of the continuous parameter change can be considered as the computational advantage of the FMM-TSOM. To prevent interference from unwanted background noise, the region of interest (ROI) around the sample position should be specified as shown in Figs. 5(a) and 6(a).

It is seen that, using the DTI and MSD calculation, the linewidth that the target sample under measurement is likely to have can be estimated at the minimum point of MSD under the reliable tolerance level of 0.1 nm. In addition, the MSD graphs and the minimum MSD point can be slightly influenced by the choice of ROI in the DTI calculation. We tested the minimum MSD point for each of a few selected ROI sizes and found that the minimum MSD estimation point can be manipulated at the sub-nanometer scale as indicated in Figs. 5(b) and 6(b).

Above all, it seems that the experimental TSOM image and the calculated reference TSOM images constructed by the proposed incoherent FMM-TSOM modeling match significantly well. The results show that the MSD of DTI can correctly indicate the position of the target sample in the database of reference TSOM images to sub-nano scale reliability. This possibility underlies the original motivation of the TSOM technology. The FMM-TSOM scheme can be meaningful for not only meteorological measurement but also the inspection measurement of such targets as single nano fin structures.

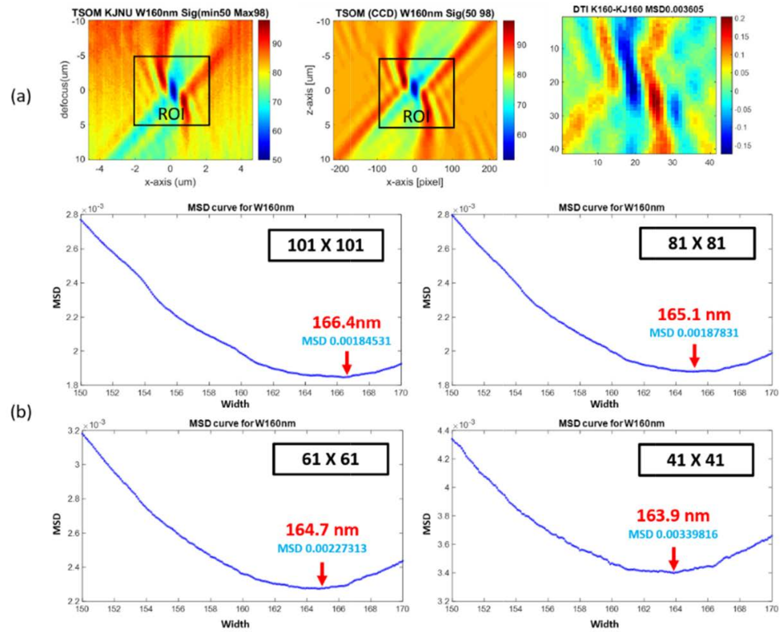


Fig. 5. (a) TSOM image for 140 nm width single line fin structure which is obtained by experiment (left) and simulation (middle), and the DTI between experiment and simulation (right). (b) Sub-nanometer scale metrology using TSOM for 140nm width under the ROI of 101x101, 81x81, 61x61, and 41x41 pixels.

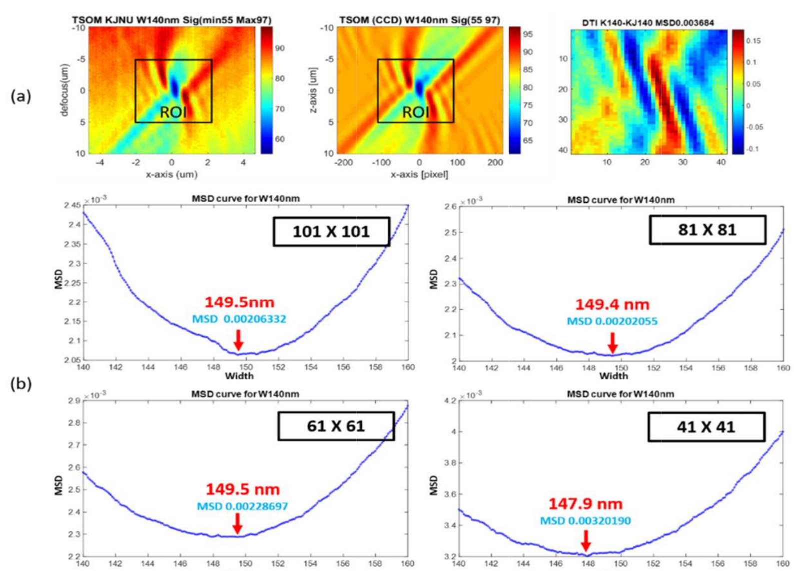


Fig. 6. (a) TSOM image for 160 nm width single line fin structure which is obtained by experiment (left) and simulation (middle), and the DTI between experiment and simulation (right). (b) Sub-nanometer scale metrology using TSOM for 160nm width under the ROI of 101x101, 81x81, 61x61, and 41x41 pixels.

## 4. Conclusion

The FMM-TSOM technique was proposed and experimentally verified. The key finding is that the careful consideration of the incoherent illumination condition, the finite NA, the incidence angle, and the cropping of the effective TSOM fingerprint region are crucial for TSOM metrology. FMM modeling is a versatile and affordable TSOM modeling algorithm that can take those key parameters into consideration. It is believed that the proposed FMM-TSOM scheme can provide an algorithmic base for the further development of commercial TSOM equipment. Nowadays, the adaptation of various advanced artificial intelligence techniques such as neural networks and deep-running algorithms are expected to prove effective for the feature extraction of sub-nanometer scale structural variation. For deep learning, a huge image database is required. Thus, the TSOM image generation engine for near continuous variation of the target structure becomes necessary. This continuous variation in structure is actually impossible in the structure representation of the spatial domain electromagnetic solver such FDTD and FEM. In contrast, the FMM does allow continuously control of the structural parameters in the spatial domain and it would be an efficient numerical method of fine TSOM image database construction for advanced artificial intelligence based TSOM inspection and metrology.

## Funding

Ministry of Trade, Industry & Energy (MOTIE) and Korea Semiconductor Research Consortium (KSRC) (10048720); National Research Foundation of Korea(NRF) (NRF-2015R1C1A1A01054652).

## Acknowledgments

Hwi Kim is the corresponding author and Junho Lee is the co-corresponding author.